Check for updates

Understanding laccase/HBT-catalyzed grass delignification at the molecular level†

Roelant Hilgers, [a] Gijs van Erven,[a] Vincent Boerkamp, [a] Irina Sulaeva,[b] Antje Potthast, [b] Mirjam A. Kabel [a] and Jean-Paul Vincken *[a]

Laccase-mediator systems (LMS) are potential green tools to improve the valorization of lignocellulosic biomass by selective degradation of lignin. Despite extensive attention devoted to lignin degradation by LMS in literature, knowledge on the underlying mechanisms is largely limited to model compound studies. Here, we report a mechanistic study on the delignification of wheat straw (WS) and corn stover (CS) by a laccase/HBT system. Quantitative ^{13}C-IS py-GC-MS analysis revealed that WS and CS were delignified in the range of 28–51% (w/w). Based on a combination of py-GC-MS, 2D NMR, SEC and RP-UHPLC-MS, extensive structural characterization of both residual and solubilized lignin structures was performed, from which we reconstructed the degradation pathway of native lignin by laccase/HBT. For the first time, we show that degradation of native lignin in the plant cell wall matrix by LMS occurs *via* both $C_\alpha-C_\beta$ cleavage and ether cleavage of β-*O*-4′ aryl ethers, and that the latter primarily occurs *via* cleavage of the β-*O* bond. C_γ-Coumaroylated substructures were found to be more recalcitrant towards degradation than non-acylated substructures. In addition to lignin degradation, our results provide evidence for grafting of HBT onto lignin.

Introduction

Agricultural by-products, such as wheat straw (WS) and corn stover (CS), are promising sources of polysaccharides for *e.g.* biochemical and biofuel production. Nevertheless, the co-occurrence of lignin in these lignocellulosic materials hinders efficient (enzymatic) conversion of the polysaccharides.[1] Hence, degradation or removal of lignin prior to polysaccharide conversion is advantageous.[2,3] Although multiple chemical and/or physical delignification strategies have been reported, most of these require harsh conditions.[2,4] Therefore, green alternatives are receiving increasing attention, such as biological pre-treatments (*e.g.* by using white-rot fungi) or fractionation with deep eutectic solvents.[5–7] Another promising approach, especially with respect to industrial applicability, is enzymatic lignin degradation.[8]

Lignin is an aromatic polymer, built up *via* polymerization of the phenylpropanoids sinapyl alcohol, coniferyl alcohol and *p*-coumaryl alcohol. When incorporated in the lignin polymer, these building blocks form syringyl (S), guaiacyl (G) and

p-hydroxyphenyl (H) subunits, respectively. Grass lignins also contain acetate, *p*-coumaric acid and ferulic acid, and also tricin may be incorporated.[9,10] Polymerization of the phenyl-propanoids results in a variety of interunit linkages, of which the β-*O*-4 linkage is the most abundant.[11] As most interunit linkages are formed *via* radical coupling of the phenolic hydroxyl groups of the phenylpropanoids, the majority (70–90%) of subunits in the lignin polymer are non-phenolic, while only 10–30% of the subunits are phenolic.[12]

Several classes of enzymes are known to be active toward lignin, including laccases and various peroxidases (*i.e.* lignin peroxidases, versatile peroxidases and manganese peroxidases). For industrial delignification of biomass, laccases are preferred to peroxidases, as laccases use molecular O_2 rather than H_2O_2 as electron acceptor, and are, in contrast to peroxidases, not inactivated by their electron acceptor.[13] Due to their relatively low redox potential (≤ 800 mV *vs.* NHE),[3] the phenolic subunits in lignin are most prone to direct laccase activity. In contrast, the non-phenolic subunits have higher redox potentials (>1400 mV),[14,15] and are, therefore, resistant to oxidation by laccase alone. Nevertheless, when laccase is combined with an appropriate mediator, its oxidizing capacity can be extended to non-phenolic lignin structures. In such a laccase-mediator system (LMS), laccase oxidizes the mediator, which subsequently undergoes a redox reaction with a (non-phenolic) lignin subunit. One of the most effective mediators known is 1-hydroxybenzotriazole (HBT).[15–17]

[a]Laboratory of Food Chemistry, Wageningen University & Research, The Netherlands. E-mail: jean-paul.vincken@wur.nl; Tel: +31 (0)317 482234
[b]Department of Chemistry, Division of Chemistry of Renewable Resources, University of Natural Resources and Life Sciences, Austria
†Electronic supplementary information (ESI) available. See DOI: 10.1039/c9gc04341a

After oxidation by the mediator, the formed lignin radical can react further *via* a variety of pathways. These pathways have, so far, mainly been investigated by using low molecular weight model compounds, resembling substructures of lignin.[18–26] Dependent on the structure of the lignin radical, bond cleavage, radical coupling and a number of other modifications have been reported, and it has been suggested that these reaction pathways are in competition with each other. Obviously, this competition determines whether LMS treatment eventually results in overall polymerization or depolymerization. Although these insights from model compound studies are valuable, so far, it remains unclear to what extent these insights can be extrapolated to LMS-induced lignin degradation *in situ*.

Over the past years, various studies have been published that report successful degradation or removal of lignin from biomass and paper pulp upon LMS treatment.[27–39] In most of these studies, however, high laccase and mediator concentrations were used, which is undesirable from both economical and sustainability perspectives. In addition, these studies focused on the effectiveness of the LMS treatments, without performing in-depth structural characterization of the LMS treated lignin. Structural characterization may reveal accumulation of both degraded and recalcitrant substructures, and thereby provide insights into the mechanisms and bottlenecks underlying LMS based delignification. These insights are essential in order to increase the efficiency of LMS based biomass delignification. Although a number of previous studies included structural characterization of LMS treated lignin (*e.g.* by 2D NMR spectroscopy), limited insights were obtained into the effect of LMS on lignin structure, due to the following reasons: (i) structural characterization was focused on the structure of residual lignin, rather than that of solubilized lignin, even in cases where lignin removal up to 50% was reported, and (ii) LMS treatments were often combined with alkaline peroxide treatments, which are known to induce structural changes in oxidized lignin.[40]

In this study, our goal was to provide more insights into the mechanisms and bottlenecks underlying LMS-induced delignification of grasses. Wheat straw and corn stover were treated with a laccase/HBT system, after which lignin fractionation and purification was performed to allow detailed characterization of both residual and solubilized lignin populations. Treatments were done at both pH 4 and 6, as the used laccase has been reported to show optimal enzyme activity at pH 4, but optimal lignin model compound oxidation in a LMS at pH 6.[41] A combination of py-GC-MS, 2D NMR, SEC and RP-UHPLC-MS was used to provide both quantitative and qualitative information on the structure of LMS treated lignin and enabled us to deduce the underlying ligninolysis mechanisms.

Experimental

Materials

Wheat straw (*Triticum aestivum*, WS) and corn stover (*Zea mays*, CS) were kindly provided by CNC (Milsbeek, The Netherlands).

Uniformly ^{13}C-labeled wheat straw lignin isolate (^{13}C-IS, 97.7 atom% [13]C) was available in our laboratory from previous research,[42] as well as 1-(3,4-dimethoxyphenyl)-3-hydroxypropan-1-one and 1-(3,4-dimethoxyphenyl)-2,3-dihydroxypropan-1-one.[43] Laccase from Trametes versicolor was purchased from Sigma Aldrich (St Louis, MO, USA) and was used without any further purification. Laccase activity was measured spectrophotometrically by oxidation of ABTS (1 U = 1 µmol oxidized ABTS min^{-1}, see ESI†). Rovabio® Advance was obtained from Adisseo (Antony, France) and ViscoStar 150L was purchased from Dyadic (Jupiter, FL, USA). All other chemicals were of analytical grade, purchased from commercial suppliers, and used without further purification. Water was purified using a MilliQ system (Millipore, Billerica, MA, USA).

Methods

Preparation of biomass for incubations. WS and CS were milled with a Centrifugal Mill ZM 200 (Retsch, Haan, Germany) (<0.7 mm), after which acetone soluble material was removed using Soxhlet extraction. Subsequently, the acetone insoluble solids were dried overnight at 20 °C, followed by 3 h at 40 °C to remove the last traces of acetone. The residues were milled by using a Retsch PM100 planetary ball mill. Hereto, a 500 mL ZrO$_2$ grinding jar was charged with 30 g of sample and 100 ZrO$_2$ balls with a diameter of 10 mm. The net milling time was 1 h at an intensity of 600 rpm. To limit overheating, a 30 min break was inserted after every 15 min of milling. It should be noted that milling in a 500 mL jar setup proceeds with a higher intensity compared to the (routine) 50 mL scale, resulting in the same extent of milling in a much shorter time. The ball-milled biomass was washed multiple times with 100–300 mL aliquots of water until nearly colorless supernatants were obtained. The water-washed residues were lyophilized to yield milled wheat straw (MWS) and milled corn stover (MCS).

Laccase-mediator treatments. Laccase/HBT treatments of MWS and MCS were performed based on the experimental conditions reported by Rencoret *et al.*[28] Samples were prepared in duplicate at pH 4 and 6 in 75 mL Parr 2890HC reactors (Parr, Moline, IL, USA). Hereto, approximately 1.5 g MWS or MCS was suspended in 25 mL 0.2 M citric acid buffer. HBT was added at a concentration of 78 mM and incubations were started by adding laccase at doses of 50 U g^{-1} MWS/MCS (pH 4 and 6) or 125 U g^{-1} MWS/MCS (only pH 6). Incubations were performed at 40 °C under magnetic stirring (550 rpm) and 2 bar O$_2$ atmosphere. After 16 h, fresh laccase was added (half of the original dose) and the samples were incubated for another 8 h under the same conditions. Additional control incubations of MWS and MCS without laccase and HBT were also performed. After a total incubation time of 24 h, the suspensions were centrifuged (4700*g*, 10 min, 20 °C). The residue was washed five times with water at a 3.75% (w/w) loading, and finally lyophilized to obtain the residue of laccase/HBT treatment (RES, see Fig. 1). The supernatants of the reaction suspensions, and the supernatants of the five washing steps were pooled and lyophilized to obtain water extractable lignin
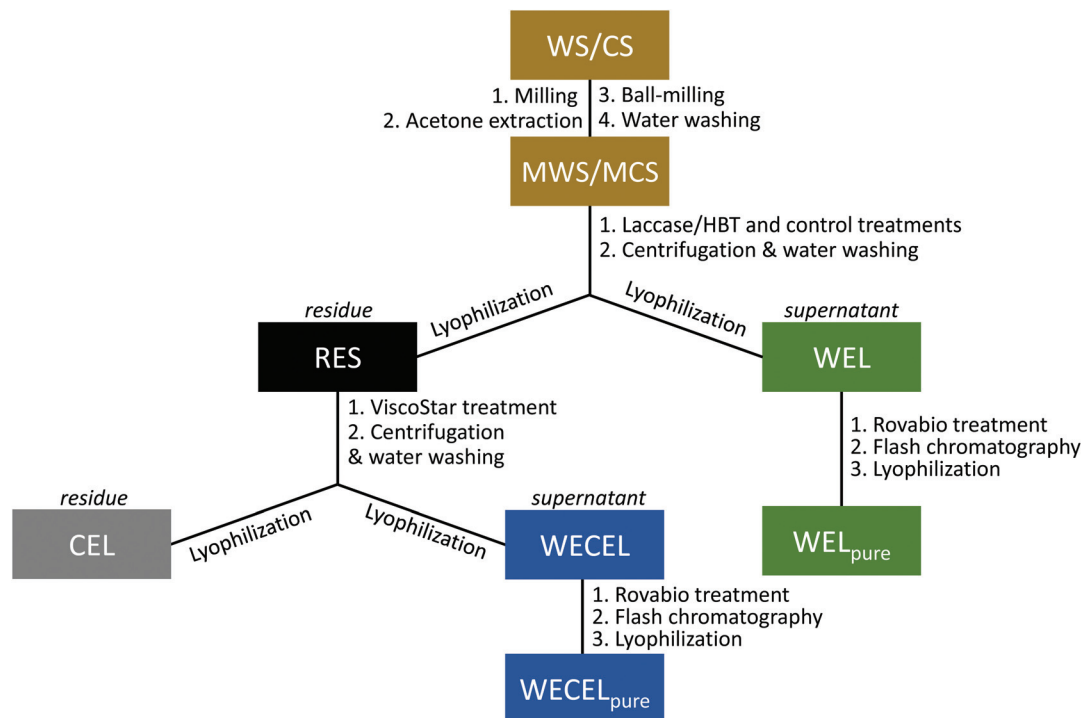
Fig. 1 Schematic overview of the incubations, fractionations and purifications in this study. (M)WS = (Milled) wheat straw; (M)CS = (Milled) corn stover; RES = residue; WEL = water-extractable lignin; CEL = cellulolytic enzyme lignin; WECEL = water-extractable cellulolytic enzyme lignin.

(WEL, Fig. 1). In addition to the above described incubations, an incubation with only laccase (3.1 U mL^{-1}) and HBT (78 mM) was performed in citric acid buffer at pH 5 (as a compromise pH) for 24 h at 40 °C. This sample was used as a control in NMR and RP-UHPLC-PDA-MS analyses.

Preparation of cellulolytic enzyme lignin (CEL) and water extractable cellulolytic enzyme lignin (WECEL). For preparation of CEL (Fig. 1), approximately 650 mg (for WS) or 550 mg (for CS) RES was suspended in sodium acetate buffer (0.05 M, pH 4.8) to a 5% (w/w) loading. Subsequently, a xylanase-enriched enzyme cocktail (ViscoStar 150L) was added to a concentration of 0.01% (w/w), obtaining a 1/500 ratio (w/w; enzyme/biomass). The suspension was incubated under rotary shaking (20 rpm) for 24 h at 50 °C, after which it was centrifuged (60 000g, 15 min, 20 °C). The residue was incubated for a second time, using fresh ViscoStar 150L and fresh buffer. The supernatant of the first incubation was stored at 4 °C. After incubation and centrifugation, the residue was washed three times with water at ~0.5% (w/w) solid loading, and lyophilized to yield cellulolytic enzyme lignin (CEL). The supernatants of both ViscoStar treatments and the supernatant from the three wash steps were combined and lyophilized to obtain water extractable cellulolytic enzyme lignin (WECEL).

Purification of WEL and WECEL. In order to remove free and lignin-bound carbohydrates, remaining HBT and related products, WECEL and WEL fractions were purified. As the amount of lignin in WEL fractions of control incubations was negligible, only WEL fractions of laccase/HBT treated WS and CS were purified. In the case of WECEL, both controls and

laccase/HBT treated samples were included. For purification, treatment duplicates of the lyophilized WECEL and WEL fractions were pooled, after which 550–600 mg WS WECEL, 450–550 mg CS WECEL and 850–1270 mg WS and CS WEL (i.e. 50% of the obtained WEL) were weighed and dissolved at 5% (w/w) solid loading in 0.2 M citric acid buffer at pH 5.5 containing 57 μg mL^{-1} of a xylanase-enriched enzyme cocktail containing also ferulic acid esterase activity (Rovabio® Advance). The solutions were incubated for 24 h at 40 °C under rotary shaking (20 rpm), and lyophilized afterwards. The dried samples were suspended in 1% (v/v) formic acid and centrifuged (4700g, 20 °C, 5 min). The pellet was washed three times with 0.5 mL 1% (v/v) formic acid. All supernatants were pooled and fractionated by using reversed phase Flash chromatography (see ESI† for detailed procedure). The purified fractions, WECEL$_{pure}$ and WEL$_{pure}$ were used for further analyses.

Quantitative ^{13}C-IS py-GC-MS. Quantification of lignin was performed by using a previously described py-GC-MS method, based on the use of a uniformly ^{13}C-labeled lignin internal standard.[42,44] In addition, the py-GC-MS data were used to fingerprint structural changes in lignin upon laccase/HBT treatment. A detailed description of the method can be found in the ESI.†

Klason lignin determination. Klason lignin determination was performed in duplicate based on a previously described method.[45] Hereto, 400 mg dried RES was weighed and 4 mL of 72% w/w sulfuric acid was added. Samples were incubated for 1 h at 30 °C, after which they were diluted with 44 mL water and incubated for 3 h at 100 °C. During both hydrolysis steps, samples were shaken and vortexed every 30 min. After hydro-

lysis, the suspensions were filtered over G4 glass filters. The residue was extensively washed with water until pH paper indicated that no residual acid was present. After drying overnight at 105 °C, the residue was weighed. The ash content (triplicates) of this residue was then determined by subjecting 1 mg portions of the sample, weighed on an XP6 excellence-plus microbalance (Mettler Toledo, Columbus, OH, USA) for 7 h to a temperature of 550 °C. The weight of the resulting residues relative to weight of the starting material (*i.e.* 1 mg) was taken as the ash content. The protein content was measured in duplicate according to the Dumas method using a Flash EA 1112 N analyzer (Thermo Scientific). Methionine was used as calibration standard, and a nitrogen to protein conversion factor of 6.25 was used. It should be noted that part of the nitrogen in laccase/HBT treated samples may have originated from HBT instead of protein. Since the contribution of HBT could not be accurately estimated, the calculated protein concentrations were reported without further correction. The acid-soluble lignin content was not determined, due to interference of UV absorption of HBT.

2D NMR spectroscopy. Structural characterization of the lignin fractions was performed by using 2D NMR analyses (HSQC and HMBC). Analysis of CEL samples was performed in gel state, based on a previously published method.[46] WECEL$_{pure}$ and WEL$_{pure}$ samples were measured in dissolved state. Detailed descriptions of the methods and integration procedures can be found in the ESI.† As no HSQC spectra of sufficient quality could be recorded for the RES fractions, relative abundances of structural features in the residue were determined based on the CEL and WECEL$_{pure}$ fractions, which were both obtained from RES. Hereto, mass-weighted averages of HSQC integrals of CEL and WECEL$_{pure}$ fractions were determined according to eqn (1):

$$\int_{res} = (M_{CEL} \times \int_{CEL} + M_{WECELpure} \times \int_{WECELpure})/(M_{CEL} + M_{WECELpure})$$

(1)

where $\int_{res}$ is the mass-weighted averaged HSQC integral for residual lignin; M_{CEL} and $M_{WECELpure}$ are the masses of lignin in the CEL and WECEL$_{pure}$ fraction, respectively; $\int_{CEL}$ and $\int_{WECELpure}$ are the HSQC integrals obtained for the CEL and WECEL$_{pure}$ fraction, respectively.

RP-UHPLC-PDA-MS. WECEL$_{pure}$ fractions were analyzed to screen for lignin–HBT coupling products. Hereto, WECEL$_{pure}$ fractions were dissolved at 1 mg mL^{-1}, centrifuged (12 500g, 5 min, 20 °C) and analyzed using RP-UHPLC-PDA-MS. A detailed description of the method can be found in the ESI.†

Size-exclusion chromatography. Size-exclusion chromatography (SEC) was performed on CEL and WECEL$_{pure}$ samples. Hereto, fractions were dissolved at 4–8 mg mL^{-1} in DMSO containing 0.5 w/v% LiBr, and were filtered through a 0.45 μm PTFE syringe filter. WECEL$_{pure}$ completely dissolved, whereas some residue was observed in the case of CEL fractions. The soluble material was analyzed by using SEC-MALS$_{(IR)}$ analysis, as described by Zinovyev *et al.*[47]

Results and discussion

Delignification of MWS and MCS

After laccase/HBT treatment of MWS and MCS, the water-washed and lyophilized residues (*i.e.* WS and CS-RES fractions) were weighed and analyzed by using quantitative py-GC-MS analysis with ^{13}C wheat straw lignin as internal standard. The analysis indicated that the laccase/HBT treatment resulted in a delignification of 44–51% and 36–44% for MWS and MCS, respectively, whereas only 0–5% delignification was observed in control incubations without laccase/HBT (Fig. 2). These values are in a similar range as those reported in a previous study on laccase/HBT based wheat straw delignification and confirm that grasses can be effectively delignified by laccase/HBT treatments.[28] The used py-GC-MS based lignin quantification method has been validated for quantification of both wheat straw and corn stover lignin,[42,44] but this was the first time the method was used for lignin quantification in LMS treated biomass. Therefore, for comparison, a Klason lignin determination was performed on the WS-RES fractions incubated at pH 4. Although the latter method suggested a MWS delignification of 32% at pH 4 (Table S5†), which is, admittedly, lower than the values obtained by using py-GC-MS, both methods show a significant decrease in lignin content after laccase/HBT treatment. As both lignin quantification methods have their drawbacks (see ESI† for a more detailed discussion), and only py-GC-MS provides additional structural information, we used this method for lignin quantification on all other samples in this study.

Although no lignin quantification could be performed for the unpurified WEL fractions,[48] it was assumed that all removed lignin ended up in the WEL fractions (see Fig. 1), as no volatile reaction products were expected to be formed.

Purification of lignin fractions

After LMS treatment, the residue (RES) and supernatant (WEL) were further fractionated and purified to facilitate structural lignin analysis by 2D NMR. Hereto, cellulolytic enzyme lignin (CEL) was prepared from RES, which resulted in a 2.0 to 2.7-
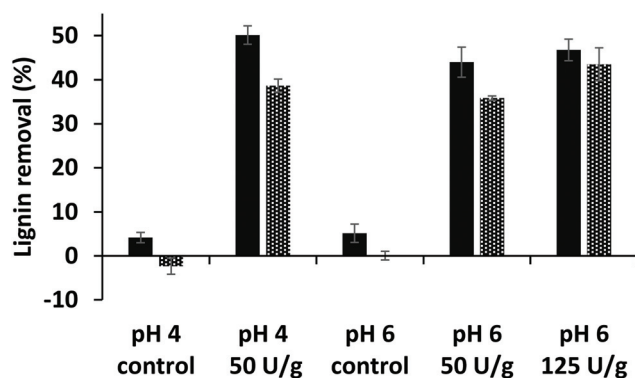
Fig. 2 Estimated lignin removal from milled wheat straw (solid bars) and milled corn stover (dotted bars) by laccase/HBT treatments based on quantitative ^{13}C-IS py-GC-MS analysis (see ESI† for details).

fold increase in lignin content (Tables S9–S12†). The resulting supernatant (WECEL) contained the released carbohydrates, but also a significant amount of lignin (*i.e.* 31–64% of the lignin originating from RES), indicating that also WECEL lignin should be analyzed for a complete overview the residual lignin structure. To facilitate analysis, WECEL was purified by treatment with a xylanase-enriched enzyme cocktail containing additional ferulic acid esterase activity, and subsequent Flash chromatography. Based on py-GC-MS analysis it was estimated that this purification increased the lignin content from ≤10.6% (w/w) in WECEL to ≥50.4% (w/w) in WECEL$_{pure}$ (Tables S13–S16†). The same strategy was used to remove sugars and mediator from WEL fractions, which resulted in WEL$_{pure}$ fractions with estimated lignin contents of 6.6–23.2% (w/w) (Table S17†). The summed lignin yields of the three final fractions (*i.e.* CEL, WECEL$_{pure}$ and WEL$_{pure}$) were estimated to be 93–100% for control incubations and 39–67% for laccase/HBT incubations (see Tables S9–S17†), though it should be noted that the yields of the laccase/HBT treated fractions are expected to be underestimations (see discussion on page S13–14).

Overall extent of lignin oxidation and degradation in CEL, WECEL$_{pure}$ and WEL$_{pure}$ fractions

As a measure for the extent of lignin oxidation in the purified WS and CS fractions (*i.e.* CEL, WECEL$_{pure}$ and WEL$_{pure}$), the relative abundance of C$_\alpha$-oxidized structures was determined based on semi-quantitative processing of 2D HSQC NMR spectra (see Fig. S1† for spectra and Table S3† for all assignments). It was observed that laccase/HBT treatment increased the relative content of C$_\alpha$-oxidized subunits in all fractions, due to oxidation of both S and G-units (Fig. 3A and Fig. S2†). The extent of C$_\alpha$-oxidation was also estimated based on the abundance of C$_\alpha$-oxidized products in py-GC-MS analysis of the same fractions (Fig. 3B). Although absolute values differed from the HSQC analysis, a very similar trend was observed: C$_\alpha$-oxidation increased in all fractions, but the extent was vastly different for each fraction. Whereas CEL fractions of laccase/

HBT treated MWS only showed 3–18% C$_\alpha$-oxidation (based on HSQC NMR), for WECEL$_{pure}$ and WEL$_{pure}$ fractions, C$_\alpha$-oxidation was 24–40% and 69–75%, respectively.

To verify that delignification of MWS and MCS was truly caused by cleavage of interunit linkages, the amount of intact interunit linkages per 100 aromatic subunits (S, G, H and oxidized analogues) was determined from the HSQC spectra. Indeed, in all fractions of laccase/HBT treated samples a decrease (up to 51%) in intact interunit linkages was observed (Fig. 4A and Fig. S3†). We also estimated the amount of interunit linkages based on the py-GC-MS data. Hereto, the relative amount of pyrolysis products with intact 3-carbon side chains (PhC$_\gamma$) were taken, after correction for cleavage markers (*i.e.* diketones and vinylketones, as shown previously).[5,43] Although the absolute values differed from those obtained using HSQC NMR, similar trends were observed (Fig. 4B). Interestingly, the amount of interunit linkages in WEL$_{pure}$ was 2–4 times lower than in CEL and WECEL$_{pure}$.

Overall, the results shown in Fig. 3 and 4 indicated that oxidized and degraded substructures accumulated in WEL$_{pure}$ (*i.e.* solubilized lignin) and to a lower extent in WECEL$_{pure}$. Consequently, analysis of only residues, as often performed in literature,[28,29,38,49] would heavily underestimate the overall effect of the laccase/HBT treatment on the structure of lignin, especially since a considerable amount of lignin is solubilized upon laccase/HBT treatment (Fig. 2).

Detailed insights into laccase/HBT induced reactions of lignin

To shed more light on the degradation pathways underlying the observed delignification, we zoomed in on the structural features of the most oxidized lignin fractions of laccase/HBT-treated MWS and MCS (*i.e.* WECEL$_{pure}$ and WEL$_{pure}$), and compared those to the structural features of the WECEL$_{pure}$ fraction of the corresponding control (Fig. 5). Although the spectra of laccase/HBT fractions showed multiple correlations that could not be annotated (grey correlations in Fig. 5), the vast majority of these correlations also occurred in spectra from the Rovabio enzyme cocktail and the control incubation contain-
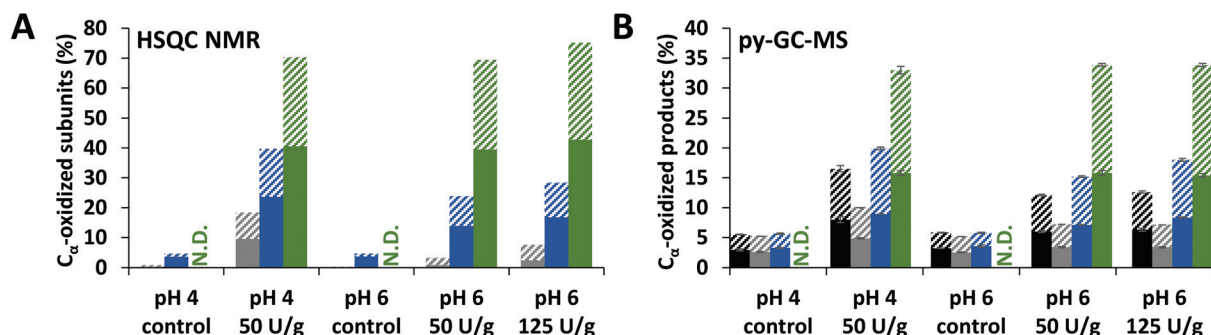

Fig. 3 Relative abundance of C$_\alpha$-oxidized subunits as determined by using HSQC NMR (A) and estimated based on py-GC-MS (B) in RES (black), CEL (grey), WECEL$_{pure}$ (blue) and WEL$_{pure}$ (green) fractions of laccase/HBT treated MWS and controls. RES was only analyzed by using py-GC-MS. Solid and striped bars correspond to G and S units, respectively. Because of their low abundance, H-units are not included. Error bars in B represent the standard deviation of two treatment duplicates and two analytical duplicates. N.D. = Not determined. C$_\alpha$-Oxidation upon treatment of MCS showed similar trends and can be found in Fig. S2.†
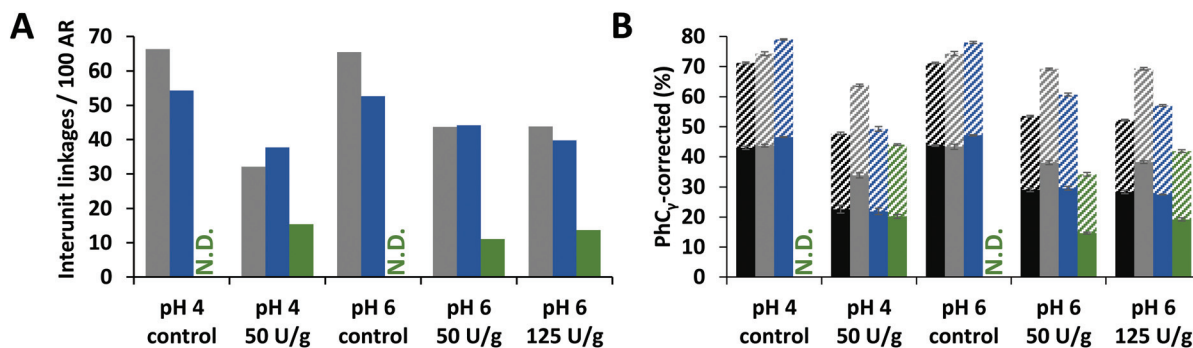
Fig. 4 HSQC NMR based (A) and py-GC-MS based (B) estimation of intact interunit linkages in RES (black), CEL (grey), WECEL_pure (blue) and WEL_pure (green) fractions of laccase/HBT treated WS and controls. RES was only analyzed by using py-GC-MS. Data corresponding to CS showed similar trends (Fig. S3†). In B, solid and striped bars refer to G and S units, respectively. Error bars in B represent the standard deviation of two treatment duplicates and two analytical duplicates. N.D. = Not determined.

ing only laccase and HBT (Fig. S5†). Thus, these correlations were mostly unrelated to lignin and were, therefore, not included in further processing of the spectra.

From the lignin-related correlations in the aliphatic region it was observed that the decreased abundance of interunit linkages upon laccase/HBT treatment (Fig. 4) was caused by a decrease in β-O-4′ linkages, as well as phenylcoumaran (β-5′) and resinol (β–β′) linkages (Fig. 5A–C). Concurrently, several new C–H correlations appeared, which were annotated based on comparison to HSQC spectra of purified degradation products of a lignin model dimer, and additional HMBC experiments (Fig. S6†). Based on these annotations, it was concluded that three new structural features appeared: (i) C_α-oxidized intact β-O-4′ linkages, (ii) hydroxypropiovanillone/syringone residues (HPV/HPS), and (iii) dihydroxy-propiovanillone/syringone residues (DHPV/S) (Fig. 5). HPV/S and DHPV/S resulted from cleavage of the β-O and O-4′ bonds of β-O-4′ linkages, respectively, and have been reported in studies on LMS-induced degradation of dimeric lignin model compounds.[19,23,25] To the best of our knowledge, our research is the first to show evidence for such degradation pathways in a LMS treatment of actual lignocellulosic biomass.

In addition to the new structural features mentioned above, one of the formed correlations (F in Fig. 5) was tentatively annotated as a cyclohexadienone ketal (CHK).[43] Such structures have been reported as products from one-electron oxidation of β-O-4′ linked model compounds,[50] but could in our study only be tentatively annotated, as no other evidence for CHK formation was found than the HSQC correlation at δ_C/δ_H 51.6/3.60.

The aromatic region also showed new C–H correlations after laccase/HBT treatment (Fig. 5D–F). In addition to C_α-oxidized S and G units, several new correlations appeared that showed overlap with HSQC correlations of HBT or its degradation products (Fig. S5†). The presence of HBT-related correlations in WECEL_pure and WEL_pure fractions could be explained by the fact that, even after purification, some residual (free) HBT and its degradation product benzotriazole (BT) were present (Table S6†). Nevertheless, as these HSQC correlations

were, with lower intensity, also visible in the laccase/HBT treated CEL fractions (Fig. S1†), and because the CEL fractions were extensively washed with water, it indicated that grafting of HBT on WS and CS lignin occurred during incubation, as has been suggested more often in literature.[51,52] Corroborating evidence for HBT grafting was found in RP-UHPLC-MS analysis of WECEL_pure fractions, which revealed the formation of reaction products that were tentatively annotated as lignin-HBT coupling products, based on their molecular formula with 3 nitrogen and ≫6 carbon atoms (Table S6†). Therefore, the grey peaks in Fig. 5E and F, likely, predominantly correspond to a combination of free, degraded and lignin-grafted HBT.

In addition to HSQC NMR, SEC-MALS_(IR) was performed on the CEL and WECEL_pure fractions to investigate the effect of the LMS treatment on the molecular weight distribution. No significant effect was observed in the case of CEL fractions. Remarkably, WECEL_pure fractions showed a slightly increased molecular weight after LMS treatment (Fig. S4†). This suggests that degradation coincided with (re)polymerization.

As lignin model compound studies have shown that, in addition to ether cleavage products, also benzoic acids could be formed (via C_α–C_β cleavage) upon LMS treatment,[23,25] and such structures would lack diagnostic correlations in HSQC spectra, we compared HMBC spectra of the WECEL_pure and WEL_pure fractions. The HMBC spectra indeed showed that, in addition to phenylketones, benzoic acids were formed upon laccase/HBT treatment, and that they were absent in the control sample (Fig. 6). In WEL_pure a small peak was also observed at δ_C 192 ppm, that was annotated as an aldehyde based on the presence of a correlation at δ_C/δ_H 192/9.8 in the corresponding HSQC spectrum (data not shown).[53] Nevertheless, as this HSQC correlation was also observed in WECEL_pure control samples, and laccase/HBT treatment did not result in more than 1 aldehyde group per 100 aromatic rings, we concluded that aldehyde formation was not a main degradation pathway during LMS treatment. Remarkably, very clear correlations were observed that corresponded to S-ketones and S-acids (δ_H 7.1–7.3), whereas the intensity of their G-analogues was very low. Possibly, G-units selectively
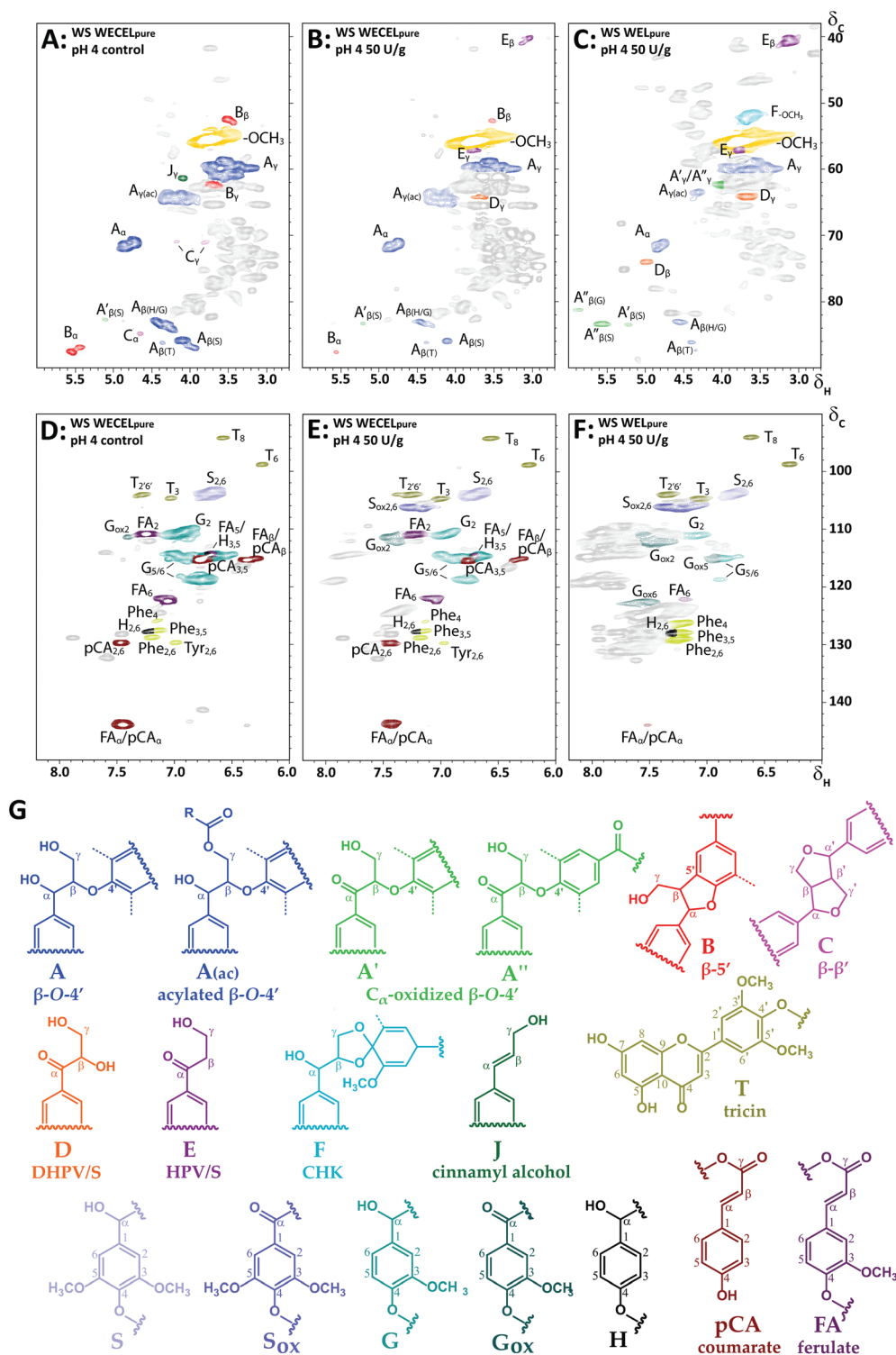
Fig. 5 Aliphatic (A–C) and aromatic (D–F) regions of HSQC spectra of (un)treated WS at pH 4: WECEL$_{pure}$ of control incubation (A & D), WECEL$_{pure}$ of laccase/HBT treatment (B & E) and WEL$_{pure}$ of laccase/HBT treatment (C & F). Lignin substructures corresponding to the colored annotations are shown in (G). Dashed lines correspond to −H or −OCH$_3$. Annotations Phe and Tyr correspond to phenylalanine and tyrosine residues, respectively. Grey correlations are unassigned signals, mainly originating from Rovabio Advance and (reaction products of) HBT. Annotation was done based on literature and by comparison with purified degradation products of a lignin model compound (see Fig. S5†).[43,56–59] Note that F is a tentative annotation, and that the displayed structure is only one of the possible cyclohexadienone structures (see van Erven *et al.* for other possible structures).[43] A complete list of annotations can be found in Table S3.† HSQC spectra of other incubations (pH 6 and CS) showed similar correlations (data not shown).
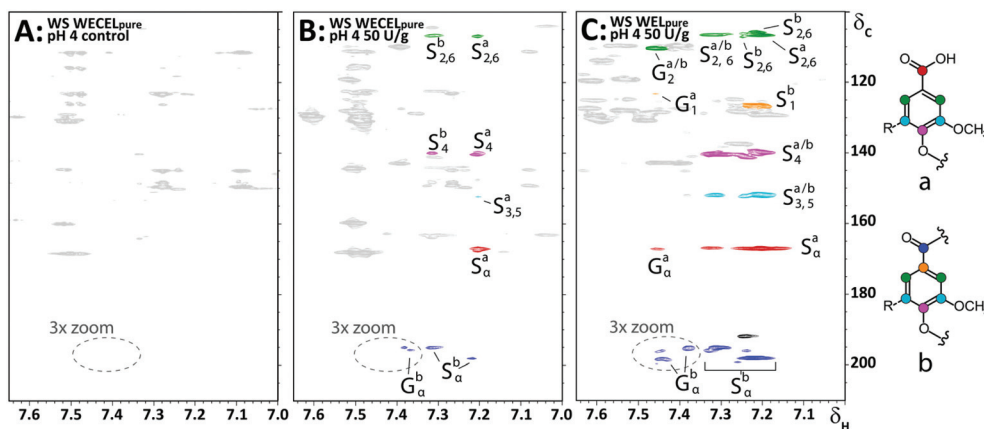
Fig. 6 Aromatic regions of $^1H-^{13}C$ HMBC spectra obtained from WECEL$_{pure}$ (A & B) and WEL$_{pure}$ (C) fractions of WS incubated at pH 4. A = control, B & C = laccase/HBT treated. Annotation was done based on comparison with reported chemical shifts of lignin model compounds.[60] The black correlation at δ_C 192 ppm in C most likely corresponds to an aldehyde, but is only present in small amounts (see main text). Substructures corresponding to the annotated correlations are shown on the right. A full 3× zoomed version of the WEL$_{pure}$ fraction, showing more ketone correlations, can be found in Fig. S7.†

undergo (re)polymerization and grafting, and that, *via* C–O coupling at C_5, this results in aromatic rings with HSQC correlations that overlap with those of S-units.[54,55] Nevertheless, this hypothesis does not match with HSQC spectra, which showed formation of both C_α-oxidized G and S units, and py-GC-MS data, which showed that the cleavage markers (*i.e.* vinyl ketones and diketones)[43] are formed from both G and S units (Tables S9–S17†). Therefore, the reason behind this discrepancy remains to be elucidated.

Relative susceptibility of lignin substructures to laccase/HBT activity

To get more insights into the relative susceptibility of lignin substructures towards degradation by laccase/HBT, lignin mass-weighted averages of the HSQC integrals of the residual lignin fractions (*i.e.* CEL and WECEL$_{pure}$) were determined (see Methods section for calculation). Based on these integrals, relative abundances of structural features in the residual lignin were calculated (Table 1). The most apparent observations are discussed below.

Firstly, Table 1 shows that, although the overall decrease in intact linkages was mainly caused by degradation of β-O-4′ linkages, the relative abundances of the interunit linkages suggested a preferential degradation of phenylcoumaran and resinol linkages. Although it is unknown whether these linkages are truly degraded or only modified, at least these findings show that not only β-O-4′ linkages, but also β-5′ and β–β′ linkages are targets of the LMS treatment.

Secondly, in all laccase/HBT treated samples the S/G ratio of the residue increased, and this has previously been suggested to result from a preferential removal of G-units.[28,29] At first sight, the increased S/G ratio indeed hints at a preferential removal of G-units, and this seems to be confirmed by the results shown in Fig. 4B and Fig. S3B,† which indicates that mainly linkages are degraded that have

their C_α atom connected to a G-unit (G-X linkage). Nevertheless, in case of preferential removal of G-units from the residue, an accumulation of G-units (low S/G ratio) is expected in the solubilized lignin. This is clearly not the case, as the S/G ratios in WEL$_{pure}$ fractions are all higher than the S/G ratios of the residual lignin (Table S7†). Another explanation for the observed increase in S/G ratio could be a higher degree of side-reactions of G-units (*e.g.* grafting and repolymerization at the C5 position), after which they may be excluded from data processing. A preferential removal of G-units and degradation of G-X linkages is therefore not proven.

Thirdly, the results shown in Table 1 indicate that *p*CA moieties accumulate in the residual lignin, in particular in CS. This accumulation is confirmed by an increased abundance of 4-vinylphenol in py-GC-MS analysis of laccase/HBT treated samples (Table S18†).[61] Hence, it was concluded that *p*CA-esterified linkages were more recalcitrant toward degradation by laccase/HBT than other linkages. This may explain the somewhat lower degree of delignification in incubations of MCS (Fig. 2), since the *p*CA content of CS is much higher than that of WS (Table 1). Extrapolating this observation to other lignocellulosic materials, it could be expected that materials with a low degree of *p*CA-acylation, such as barley straw and rye straw,[62] are better targets for LMS based delignification strategies than highly *p*CA-acylated materials like sugarcane bagasse.[58]

Lastly, a remarkable pH effect was observed for the degradation of tricin after laccase/HBT treatment. Whereas the relative abundance of tricin remained unaltered at pH 4, a decrease was observed at pH 6. As no accumulation of tricin was observed in the WEL$_{pure}$ fraction, tricin was truly degraded, rather than only solubilized.

In summary, these insights show that the laccase/HBT acts on a broad range of lignin substructures, and that the relative

Table 1 Structural features of residual lignin after laccase/HBT and control treatments as measured by HSQC NMR. Values displayed in this table are lignin mass-weighted averaged values from CEL and WECEL$_{pure}$ fractions (see Methods section for calculation). Structural features of lignin in WEL$_{pure}$ fractions can be found in Table S7†

	Wheat straw					Corn stover				
	pH 4		pH 6			pH 4		pH 6		
Laccase (U g^{-1})	0	50	0	50	125	0	50	0	50	125
Lignin subunits (%)										
H	3	3	3	3	3	3	5	3	4	4
G	64	37	65	51	48	58	40	59	50	49
G$_{ox}$	1	19	1	8	11	5	13	4	7	9
S	31	28	31	31	30	34	32	34	32	32
S$_{ox}$	1	13	1	7	9	1	10	0	7	6
S/G	0.48	0.75	0.47	0.63	0.66	0.57	0.81	0.57	0.68	0.67
Hydroxycinnamates^a										
pCA	10	11	10	11	11	69	98	68	87	86
FA	26	22	27	19	19	74	28	72	22	26
Flavonoids^a										
Tricin	10	10	15	7	6	6	6	8	4	4
Interunit linkages^{a,b}										
β-O-4′ (A)	52 (82)	28 (82)	51 (82)	42 (85)	38 (84)	46 (91)	27 (92)	40 (91)	30 (88)	23 (88)
β-O-4′$_{ox}$ (A′/A″)	1 (2)	4 (12)	2 (3)	2 (5)	2 (4)	1 (1)	1 (2)	1 (1)	3 (7)	1 (5)
β-5′ (B)	8 (13)	2 (6)	8 (12)	4 (9)	5 (10)	4 (7)	2 (6)	3 (8)	2 (5)	2 (8)
β–β′ (C)	2 (3)	0 (0)	2 (3)	1 (2)	1 (2)	0 (0)	0 (0)	0 (0)	0 (0)	0 (0)
Total (100%)	63	35	63	50	46	50	29	44	35	26
Cleavage products^a										
DHPV/DHPS (D)	0.0	0.7	0.0	0.0	0.2	0.0	0.0	0.0	0.0	0.0
HPV/HPS (E)	0.3	3.4	0.0	1.0	1.4	0.0	0.6	0.0	0.5	0.8

^{a} Amount of linkages per 100 aromatic units (S + S$_{ox}$ + G + G$_{ox}$ + H). ^{b} Numbers between brackets refer to relative abundance.

susceptibility is dependent on both the local structure of lignin and the reaction conditions.

Mechanisms underlying grass delignification by laccase/HBT

Overall, our results indicate that the β-O-4′ linkages of MWS and MCS lignin undergo four types of reactions in laccase/HBT treatments: (i) C$_\alpha$–C$_\beta$ cleavage, yielding carboxylic acid residues (route A in Fig. 7); (ii) O-4′ cleavage, yielding DHPV/S residues (route B in Fig. 7); (iii) β-O cleavage, yielding HPV/S residues (route C in Fig. 7); and C$_\alpha$ oxidation of intact linkages (route D in Fig. 7). As HPV/S residues and C$_\alpha$-oxidized β-O-4′ linkages are formed to a much larger extent than DHPV/S residues (Table 1 and Table S7†), we concluded that C$_\alpha$-oxidation and β-O cleavage are the major reactions induced by laccase/HBT treatments and that O-4′ cleavage only occurs to a minor extent. A quantitative comparison between these pathways and C$_\alpha$–C$_\beta$ cleavage was not possible, as benzoic acids (formed *via* C$_\alpha$–C$_\beta$ cleavage) lacked diagnostic HSQC correlations.

Lignin oxidation by HBT radicals is generally suggested to occur *via* hydrogen atom transfer (HAT), which results in the formation of benzylic radicals.[14] The formation of carboxylic acids, HPV/S and C$_\alpha$-oxidized linkages can, indeed, be explained from benzylic radical intermediates (Fig. 7). The formation of DHPV/S, however, is more likely to occur *via* a radical cation intermediate. The latter is formed *via* direct electron transfer (ET), rather than HAT. Although the redox potentials of non-phenolic lignin subunits (>1.4 V *vs.* NHE)[14,15] are higher than that of HBT (1.08 V *vs.* NHE),[15] a slow ET between HBT radicals and non-phenolic lignin subunits with relatively low redox potentials seems plausible, and has been suggested more often.[23] Since S-units have a lower redox potential than G-units, due to the presence of an extra methoxyl group, it is expected that O-4′ cleavage preferentially occurs in β-O-4′ linkages with a 4′-linked S-unit. Route B in Fig. 7 could, in theory, also occur *via* one-electron oxidation of C$_\alpha$-oxidized structures and subsequent cleavage. Since we found that a C$_\alpha$-oxidized lignin dimer (veratrone) was inert to the laccase/HBT system (data not shown), we consider the mechanism displayed in Fig. 7 more plausible. Considering that we observed that C$_\alpha$-oxidation and β-O cleavage were more predominant than O-4′ cleavage, our results confirm that HAT is the main oxidation mechanism underlying lignin degradation by laccase/HBT.

Upon cleavage of β-O-4′ linkages, phenoxyl radicals are expected to be formed.[23] We suggest that these radicals undergo coupling (grafting) to HBT radicals present in solution. This is further evidenced by model compound studies, in which HBT-coupling was observed with phenoxyl radicals, and not with benzylic radicals.[18,19] In addition to HBT grafting, phenoxyl radicals may also undergo radical coupling to other lignin-derived radicals (repolymerization).[18,63] Although no NMR based evidence could be obtained for this, SEC results indeed suggested that (re)polymerization of lignin occurred (Fig. S4†).
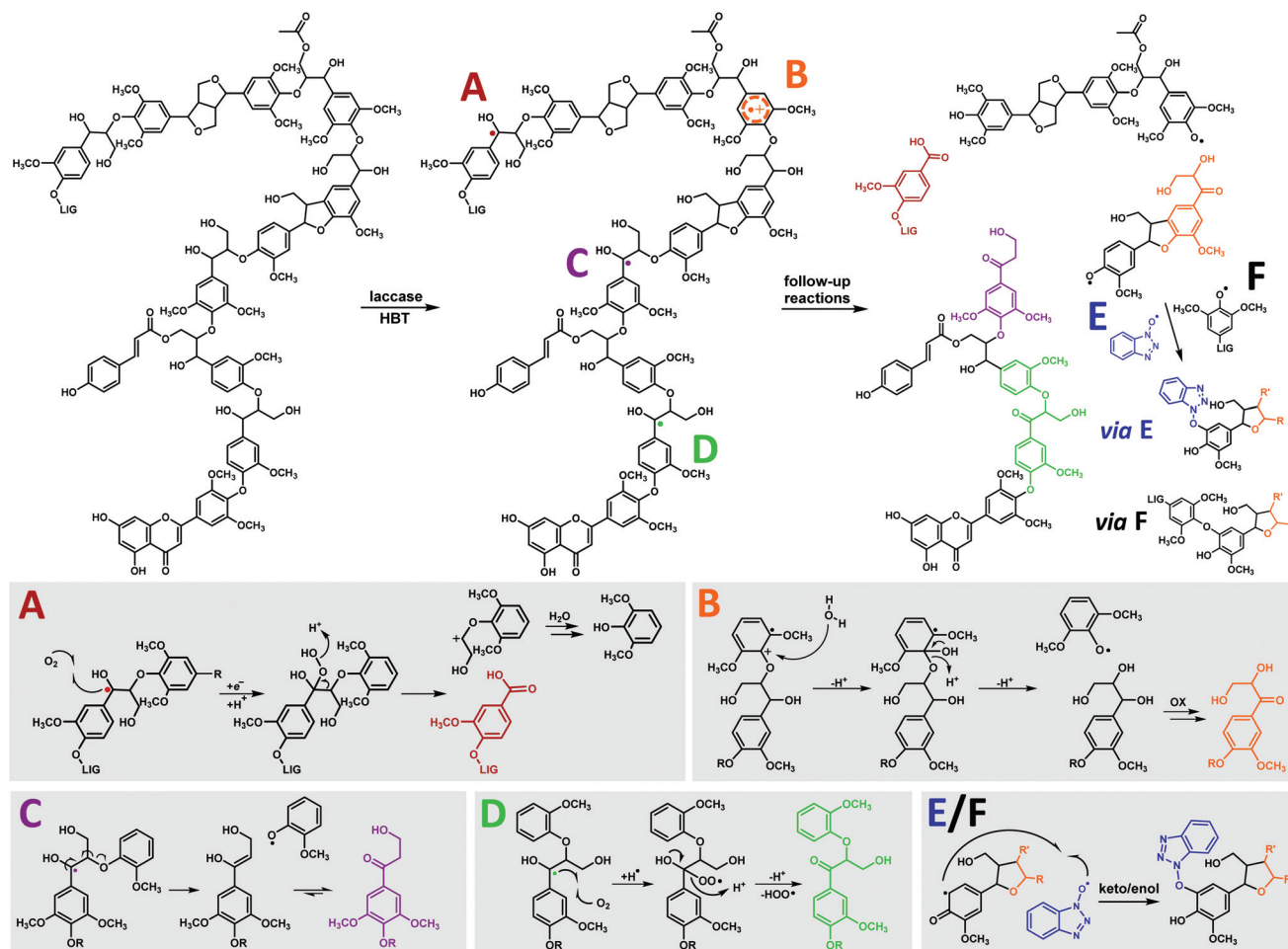
Fig. 7 General overview of the observed structural changes upon laccase/HBT treatment of MWS and MCS and suggested corresponding reactions mechanisms, shown on substructures of the lignin structure in the upper panel. A = C_α–C_β cleavage, B = O-4′ cleavage, C = β-O cleavage, D = C_α oxidation, E = HBT grafting and F = repolymerization. As E and F are expected to follow similar mechanisms, only reaction E is completely shown. Mechanisms are based on model compound studies in literature.[18,23,63,64] Degradation pathways of β-5′ and β–β′ linkages are not distinctly shown due to their low abundance.

The insights presented in this study can be used as a starting point for further optimization of lignin degradation by LMS. Our results indicated that the presence of esterified *p*CA decreases the susceptibility of linkages toward degradation by LMS. Therefore, removal of *p*CA esters, either during a pre-treatment step or simultaneously with LMS treatment, is expected to increase LMS-induced lignin degradation. A green approach for *p*CA removal could be the addition of feruloyl or coumaroyl esterases.[65,66]

we showed that β-O-4′ ether cleavage predominantly occurs *via* cleavage of the β-O bond, rather than the O-4′ bond. Furthermore, our findings suggested that *p*CA-esterification decreased the susceptibility of linkage degradation in lignin and that HBT grafts onto lignin. These mechanistic insights contribute to the fundamental understanding of enzymatic lignin degradation and can be used to optimize lignin degradation by LMS or comparable treatments in the future.

Conclusions

By fractionation, purification and comprehensive analysis of laccase/HBT treated milled wheat straw (MWS) and milled corn stover (MCS), we were able to elucidate laccase/HBT induced delignification pathways. We have shown that laccase/HBT treatment successfully degrades lignin in MWS and MCS, *via* both ether cleavage and C_α–C_β cleavage. For the first time,

Conflicts of interest

There are no conflicts to declare.

Acknowledgements

Notes and references

1 S. D. Mansfield, C. Mooney and J. N. Saddler, *Biotechnol. Prog.*, 1999, **15**, 804–816.

2 L. P. Christopher, B. Yao and Y. Ji, *Front. Energy Res.*, 2014, **2**, 12.

3 L. Munk, A. K. Sitarz, D. C. Kalyani, J. D. Mikkelsen and A. S. Meyer, *Biotechnol. Adv.*, 2015, **33**, 13–24.

4 S. Behera, R. Arora, N. Nandhagopal and S. Kumar, *Renewable Sustainable Energy Rev.*, 2014, **36**, 91–106.

5 G. Van Erven, N. Nayan, A. S. M. Sonnenberg, W. H. Hendriks, J. W. Cone and M. A. Kabel, *Biotechnol. Biofuels*, 2018, **11**, 262.

6 J. L. Mamilla, U. Novak, M. Grilc and B. Likozar, *Biomass Bioenergy*, 2019, **120**, 417–425.

7 D. L. Gall, J. Ralph, T. J. Donohue and D. R. Noguera, *Curr. Opin. Biotechnol.*, 2017, **45**, 120–126.

8 A. T. Martinez, F. J. Ruiz-Duenas, M. J. Martinez, J. C. del Río and A. Gutierrez, *Curr. Opin. Biotechnol.*, 2009, **20**, 348–357.

9 J. Ralph, C. Lapierre and W. Boerjan, *Curr. Opin. Biotechnol.*, 2019, **56**, 240–249.

10 J. Ralph, K. Lundquist, G. Brunow, F. Lu, H. Kim, P. F. Schatz, J. M. Marita, R. D. Hatfield, S. A. Ralph and J. H. Christensen, *Phytochem. Rev.*, 2004, **3**, 29–60.

11 R. Vanholme, B. Demedts, K. Morreel, J. Ralph and W. Boerjan, *Plant Physiol.*, 2010, **153**, 895–905.

12 K. Lundquist and J. Parkås, *BioResources*, 2011, **6**, 920–926.

13 D. M. Mate and M. Alcalde, *Microb. Biotechnol.*, 2017, **10**, 1457–1467.

14 P. Baiocco, A. M. Barreca, M. Fabbrini, C. Galli and P. Gentili, *Org. Biomol. Chem.*, 2003, **1**, 191–197.

15 M. Fabbrini, C. Galli and P. Gentili, *J. Mol. Catal. B: Enzym.*, 2002, **16**, 231–240.

16 F. d'Acunzo and C. Galli, *Eur. J. Biochem.*, 2003, **270**, 3634–3640.

17 P. Astolfi, P. Brandi, C. Galli, P. Gentili, M. F. Gerini, L. Greci and O. Lanzalunga, *New J. Chem.*, 2005, **29**, 1308–1317.

18 R. J. Hilgers, J.-P. Vincken, H. Gruppen and M. A. Kabel, *ACS Sustainable Chem. Eng.*, 2018, **6**, 2037–2046.

19 R. Hilgers, M. Twentyman-Jones, A. van Dam, H. Gruppen, H. Zuilhof, M. A. Kabel and J.-P. Vincken, *Catal. Sci. Technol.*, 2019, **9**, 1535–1542.

20 S. Kawai, M. Asukai, N. Ohya, K. Okita, T. Ito and H. Ohashi, *FEMS Microbiol. Lett.*, 1999, **170**, 51–57.

21 S. Kawai, T. Umezawa and T. Higuchi, *Arch. Biochem. Biophys.*, 1988, **262**, 99–110.

22 S. Kawai, M. Nakagawa and H. Ohashi, *FEBS Lett.*, 1999, **446**, 355–358.

23 S. Kawai, M. Nakagawa and H. Ohashi, *Enzyme Microb. Technol.*, 2002, **30**, 482–489.

24 A. Potthast, T. Rosenau, H. Koch and K. Fischer, *Holzforschung*, 1999, **53**, 175–180.

25 E. Srebotnik and K. E. Hammel, *J. Biotechnol.*, 2000, **81**, 179–188.

26 R. Bourbonnais, M. Paice, B. Freiermuth, E. Bodie and S. Borneman, *Appl. Environ. Microbiol.*, 1997, **63**, 4627–4632.

27 A. Rico, J. Rencoret, J. C. Del Río, A. T. Martínez and A. Gutiérrez, *BioEnergy Res.*, 2015, **8**, 211–230.

28 J. Rencoret, A. Pereira, J. C. Del Río, A. T. Martínez and A. Gutiérrez, *BioEnergy Res.*, 2016, **9**, 917–930.

29 A. Rico, J. Rencoret, J. C. Del Río, A. T. Martínez and A. Gutiérrez, *Biotechnol. Biofuels*, 2014, **7**, 6.

30 S. Camarero, D. Ibarra, Á. T. Martínez, J. Romero, A. Gutiérrez and J. C. Del Río, *Enzyme Microb. Technol.*, 2007, **40**, 1264–1271.

31 X. Du, J. Li, G. Gellerstedt, J. Rencoret, J. C. Del Río, A. T. Martínez and A. Gutiérrez, *Biomacromolecules*, 2013, **14**, 3073–3080.

32 Q. Chen, M. N. Marshall, S. M. Geib, M. Tien and T. L. Richard, *Bioresour. Technol.*, 2012, **117**, 186–192.

33 Z. Zheng, H. Li, L. Li and W. Shao, *Biotechnol. Lett.*, 2012, **34**, 541–547.

34 E. D. Babot, A. Rico, J. Rencoret, L. Kalum, H. Lund, J. Romero, J. C. Del Rio, Á. T. Martínez and A. Gutiérrez, *Bioresour. Technol.*, 2011, **102**, 6717–6722.

35 A. G. Barneto, E. Aracri, G. Andreu and T. Vidal, *Bioresour. Technol.*, 2012, **112**, 327–335.

36 D. Moldes, M. Díaz, T. Tzanov and T. Vidal, *Bioresour. Technol.*, 2008, **99**, 7959–7965.

37 D. Moldes, E. Cadena and T. Vidal, *Bioresour. Technol.*, 2010, **101**, 6924–6929.

38 J. Rencoret, A. Pereira, J. C. Del Río, A. T. Martínez and A. Gutiérrez, *ACS Sustainable Chem. Eng.*, 2017, **5**, 7145–7154.

39 J. Rencoret, A. Pereira, G. Marques, J. C. Del Río, Á. T. Martínez and A. Gutiérrez, *Holzforschung*, 2018, **73**, 45–54.

40 J. Gierer, F. Imsgard and I. Noren, *Acta Chem. Scand., Ser. B*, 1977, **31**, 561–572.

41 T. Rosado, P. Bernardo, K. Koci, A. V. Coelho, M. P. Robalo and L. O. Martins, *Bioresour. Technol.*, 2012, **124**, 371–378.

42 G. Van Erven, R. De Visser, D. W. H. Merkx, W. Strolenberg, P. De Gijsel, H. Gruppen and M. A. Kabel, *Anal. Chem.*, 2017, **89**, 10907–10916.

43 G. Van Erven, R. J. Hilgers, P. De Waard, E.-J. Gladbeek, W. J. H. Van Berkel and M. A. Kabel, *ACS Sustainable Chem. Eng.*, 2019, **7**, 16757–16764.

44 G. Van Erven, R. De Visser, P. De Waard, W. J. H. Van Berkel and M. A. Kabel, *ACS Sustainable Chem. Eng.*, 2019, **7**, 20070–20076.

45 E. Jurak, A. M. Punt, W. Arts, M. A. Kabel and H. Gruppen, *PLoS One*, 2015, **10**, e0138909.

46 S. D. Mansfield, H. Kim, F. Lu and J. Ralph, *Nat. Protoc.*, 2012, **7**, 1579.

47 G. Zinovyev, I. Sulaeva, S. Podzimek, D. Rössner, I. Kilpeläinen, I. Sumerskii, T. Rosenau and A. Potthast, *ChemSusChem*, 2018, **11**, 3259–3268.

48 Unpurified WEL fractions were expected to have a very high content of HBT, which is explosive in unhydrated form, and therefore unsuitable for pyrolysis.

49 R. Martin-Sampedro, E. A. Capanema, I. Hoeger, J. C. Villar and O. J. Rojas, *J. Agric. Food Chem.*, 2011, **59**, 8761–8769.

50 S. Kawai, T. Umezawa and T. Higuchi, *FEBS Lett.*, 1987, **210**, 61–65.

51 T. Jestel, S. Roth, D. Heesel, A. Kress, R. Fischer and A. C. Spiess, *Biocatal. Biotransform.*, 2019, **37**, 66–76.

52 L. Munk, A. M. Punt, M. A. Kabel and A. S. Meyer, *RSC Adv.*, 2017, **7**, 3358–3368.

53 A. F. Martin, Y. Tobimatsu, R. Kusumi, N. Matsumoto, T. Miyamoto, P. Y. Lam, M. Yamamura, T. Koshiba, M. Sakamoto and T. Umezawa, *Sci. Rep.*, 2019, **9**, 1–14.

54 Y. Li, T. Akiyama, T. Yokoyama and Y. Matsumoto, *Biomacromolecules*, 2016, **17**, 1921–1929.

55 F. Yue, F. Lu, S. Ralph and J. Ralph, *Biomacromolecules*, 2016, **17**, 1909–1920.

56 J. Zeng, G. L. Helms, X. Gao and S. Chen, *J. Agric. Food Chem.*, 2013, **61**, 10848–10857.

57 J. C. Del Río, J. Rencoret, P. Prinsen, A. T. Martínez, J. Ralph and A. Gutiérrez, *J. Agric. Food Chem.*, 2012, **60**, 5922–5935.

58 J. C. Del Río, A. G. Lino, J. L. Colodette, C. F. Lima, A. Gutiérrez, Á. T. Martínez, F. Lu, J. Ralph and J. Rencoret, *Biomass Bioenergy*, 2015, **81**, 322–338.

59 H. Guo, D. M. Miles-Barrett, A. R. Neal, T. Zhang, C. Li and N. J. Westwood, *Chem. Sci.*, 2018, **9**, 702–711.

60 S. A. Ralph, J. Ralph and L. Landucci, 2009, available at URL http://www.glbrc.org/databases_and_software/nmrdatabase/.

61 In the py-GC-MS analysis, 4-vinylphenol was used as a marker for the abundance of *p*-coumaric acid. Although also pyrolysis of H-units may contribute to the formation of 4-vinylphenol, this contribution is expected to be minor as the abundance of H-units in the WS and CS fractions was very low (≤5%).

62 R. Sun, X. Sun, S. Wang, W. Zhu and X. Wang, *Ind. Crops Prod.*, 2002, **15**, 179–188.

63 B. Ramalingam, B. Sana, J. Seayad, F. Ghadessy and M. Sullivan, *RSC Adv.*, 2017, **7**, 11951–11958.

64 R. Ten Have and P. J. Teunissen, *Chem. Rev.*, 2001, **101**, 3397–3414.

65 I. Benoit, D. Navarro, N. Marnet, N. Rakotomanomana, L. Lesage-Meessen, J.-C. Sigoillot, M. Asther and M. Asther, *Carbohydr. Res.*, 2006, **341**, 1820–1827.

66 W. S. Borneman, L. Ljungdahl, R. Hartley and D. Akin, *Appl. Environ. Microbiol.*, 1991, **57**, 2337–2344.